Cells Tissues Organs

Cells Tissues Organs 2011;194:188–193
DOI: 10.1159/000324827

Published online: May 13, 2011

Potential Role of the Amelogenin N-Terminus in the Regulation of Calcium Phosphate Formation in vitro

E. Le Norcy[a] S.-Y. Kwak[a] F.B. Wiedemann-Bidlack[a] E. Beniash[b] Y. Yamakoshi[c] J.P. Simmer[c] H.C. Margolis[a]

[a]Department of Biomineralization, The Forsyth Institute, Cambridge, Mass., [b]Department of Oral Biology, University of Pittsburgh, Pittsburgh, Pa., and [c]Department of Biologic and Materials Sciences, University of Michigan School of Dentistry, Ann Arbor, Mich., USA

Key Words
Amelogenin · Calcium phosphates · Enamel · LRAP · Mineralization

Abstract
N-terminal and C-terminal (CT) domains of amelogenin have been shown to be essential for proper enamel formation. Recent studies have also suggested that although the C-terminus plays an apparent role in protein-mineral interactions, other amelogenin structural domains are involved. The objective was to explore the role of the amelogenin N-terminus in the regulation of calcium phosphate formation in vitro. Spontaneous mineralization studies were carried out using the phosphorylated (+P) and nonphosphorylated (–P) N-terminus of the leucine-rich amelogenin peptide (LRAP) that lacks the hydrophilic CT domain. Mineralization progress was monitored via changes in solution pH. Mineral phases formed were characterized using TEM, selected area electron diffraction, and FT-IR. In controls, amorphous calcium phosphate was initially formed and subsequently transformed to randomly oriented hydroxyapatite (HA) plate-like crystals. In contrast to the control, LRAP(+P)-CT stabilized ACP formation for >1 day, while LRAP(–P)-CT accelerated the transformation of ACP to HA but had little effect on crystal shape or orientation. In conclusion, the N-terminal domain found in LRAP, as in amelogenins, appears to have the capacity to interact with forming calcium phosphate mineral phases. Results suggest that the N-terminal domain of amelogenin may play a direct role in early stages of enamel formation.

Copyright © 2011 S. Karger AG, Basel

Introduction

Amelogenin comprises more than 90% of the enamel matrix [Termine et al., 1980; Fincham et al., 1999] and is essential for normal enamel development [Gibson et al., 2001]. Two non-amelogenin enamel matrix proteins, i.e. enamelin and ameloblastin, have also been shown to play

Abbreviations used in this paper

ACP	amorphous calcium phosphate
FT-IR	Fourier transform-infrared spectroscopy
LRAP	leucine-rich amelogenin peptide
NMR	nuclear magnetic resonance spectroscopy
SAED	selected area electron diffraction
TEM	transmission electron microscopy

KARGER

Fax +41 61 306 12 34
E-Mail karger@karger.ch
www.karger.com

© 2011 S. Karger AG, Basel

Accessible online at:
www.karger.com/cto

Dr. Henry C. Margolis
Department of Biomineralization
The Forsyth Institute
245 First Street, Cambridge, MA 02142 (USA)
Tel. +1 617 892 8346, E-Mail hmargolis@forsyth.org

critical roles in enamel formation [Fukumoto et al., 2004; Hu et al., 2008; Wazen et al., 2009] despite the fact that they are present in relatively low proportions. Although the precise functional role of each of these proteins in enamel formation is not fully understood [Smith et al., 2009], the predominant enamel matrix protein, amelogenin, is believed to play a direct role in guiding the formation of ordered arrays of initially formed thin ribbons of apatitic crystals during the secretory phase of amelogenesis [Margolis et al., 2006]. These ordered arrays serve as a template for the rod structure of mature enamel. Amelogenin is a relatively hydrophobic protein that is comprised of 3 domains: an N-terminal tyrosine-rich domain (TRAP) that contains the only phosphorylated site in the molecule, a large central hydrophobic domain, and a charged hydrophilic C-terminus. Soon after secretion, amelogenin is cleaved through selective proteolysis from the C-terminal end [Bartlett and Simmer, 1999]. However, the full-length molecule is exclusively associated with initially formed enamel mineral [Uchida et al., 1991], suggesting that it plays a unique role in regulating this process. Transgenic studies have also revealed that both the N-terminal and the C-terminal domains of amelogenin are essential for proper enamel formation [Paine and Snead, 1997; Paine et al., 2003a; Paine et al., 2003b; Pugach et al., 2010]. In vitro studies from our laboratory have shown that full-length amelogenin can guide the formation of ordered arrays of apatitic crystals under specified conditions and that this ability is dependent on the presence of the hydrophilic C-terminus [Kwak et al., 2009].

The findings noted above, along with additional results from adsorption [Moradian-Oldak et al., 2002; Shaw et al., 2004] and seeded crystal growth [Aoba et al., 1987; Moradian-Oldak et al., 1998] studies, have also suggested that amelogenin-mineral interactions are promoted through the hydrophilic C-terminus. Recent solid-state nuclear magnetic resonance (NMR) studies, however, using the leucine-rich amelogenin peptide (LRAP), a product of alternative splicing of the amelogenin from mouse that is comprised of 59 amino acids, and the 33 N-terminal (including the phosphorylation site) and the 26 C-terminal amino acids (including the hydrophilic domain) of the full-length (180 amino acid) amelogenin isoform, have indicated that other regions of this molecule also contribute to LRAP binding to hydroxyapatite [Shaw et al., 2008; Shaw and Ferris, 2008]. Based on these findings and recent data from our laboratory that show that the single phosphate group located on serine-16 in the N-terminal domain of native amelogenins has a significant influence on mineralization [Kwak et al., 2009], the present study was undertaken to explore the effect of the N-terminal domain of LRAP on spontaneous calcium phosphate formation in vitro.

Materials and Methods

Preparation of Amelogenin Peptides

Phosphorylated [LRAP(+P)-CT] and nonphosphorylated [LRAP(–P)-CT] forms of the N-terminal domain of porcine LRAP (56 amino acids) that lack the 16 C-terminal hydrophilic amino acid domain (fig. 1) were synthesized commercially (NEO Peptide, Cambridge, Mass., USA) and purified as previously described [Nagano et al., 2009]. Lyophilized peptides were weighed and dissolved in distilled deionized water at room temperature to yield stock solutions of 5 mg/ml. Solutions were kept at room temperature for 30 min and then stored at 4°C for 24 h before checking complete dissolution by dynamic light scattering. Peptide stock solutions were centrifuged (10,900 × *g* at 4°C for 20 min) just prior to use. All other solutions were first passed through a 0.22-μm filter.

Mineralization Studies

Aliquots of calcium and pH-adjusted phosphate solution (pH 11.0) were sequentially added to peptide solutions as previously reported [Kwak et al., 2009]. The solution was quickly adjusted to pH 7.4 at 37°C with small quantities of KOH to yield final concentrations of 2.5 mM Ca, 1.5 mM P, and 2 mg/ml peptide (final volume 0.06 ml). The pH of each experimental solution was monitored continuously using a microcombination pH electrode (MI-410; Microelectrodes Inc., Bedford, N.H., USA). A duplicate sample was also prepared and used solely for transmission electron microscopy (TEM) analyses, as described below. The final pH of the latter sample was checked to confirm that it was similar to that of the other sample. A minimum of 3 experiments were carried out for each peptide and the control.

TEM Analyses

Five-microliter aliquots were taken at specific time points from mineralization samples and placed on carbon-coated Cu grids (Electron Microscopy Sciences, Hartfield, Pa., USA). Grids were prepared in duplicate. Images were obtained from duplicate grids prepared from a minimum of 3 different experiments in bright-field and selected area electron diffraction (SAED) modes using a JEOL 1200 TEM microscope at 100 kV and captured by an AMT CCD camera (AMT, Danvers, Mass., USA). The images were analyzed using ImageJ 1.43u software (NIH, USA).

Fourier Transform-Infrared Spectroscopic Analyses

Following selected mineralization experiments, 24-hour samples were concentrated, placed on a KBr IR Card (International Crystal Labs, Garfield, N.J., USA), and air-dried. The Fourier transform-infrared (FT-IR) spectra (4,000–450 cm^{-1}) of samples were recorded using a Multiscope FT-IR microscope (Perkin-Elmer) as previously reported [Kwak et al., 2009].

P173	MPLPPHPGHPGYINF***S*^P^**YEVLTPLKWYQNMIRHP-#-SLLPDLPLEAWP**ATDKTKREEVD**
	hydrophilic domain
LRAP	MPLPPHPGHPGYINF***S*^P^**YEVLTPLKWYQNMIRHPSLLPDLPLEAWP**ATDKTKREEVD**
LRAP(+P)-CT	MPLPPHPGHPGYINF***S*^P^**YEVLTPLKWYQNMIRHPSLLPDLP**----------
LRAP(–P)-CT	MPLPPHPGHPGYINF***S*****YEVLTPLKWYQNMIRHPSLLPDLP**----------

Fig. 1. Partial amino acid sequence of full-length native porcine amelogenin P173 and the indicated relationship to the synthetic forms of LRAP used. The central hydrophobic domain of P173 (indicated by #) is not shown to emphasize the relationship of P173 to the LRAP variants.

Results

The effect of the phosphorylated [LRAP(+P)-CT] and nonphosphorylated [LRAP(–P)CT] forms of LRAP on the rate of spontaneous calcium phosphate precipitation in vitro was monitored through changes in pH. In the absence of peptide (control), a marked decrease in pH was observed as a function of time (fig. 2). An initial plateau (~pH 7.2) was seen until ~30 min and corresponded to the presence of dispersed spherical particles of amorphous calcium phosphate (ACP) as described below. Mineral phase identification was based on SAED analysis and TEM observations (fig. 3a, 30 min, inset), which were consistent with amorphous material and the known morphology of ACP [Eanes, 2001; Mahamid et al., 2008]. A marked decrease in pH was then observed that corresponded to the formation and growth of plate-like particles at 4 h (fig. 3a, 4 h) followed by a slow decrease in pH up to 1,400 min (~24 h), at which point randomly oriented rhombohedral or rounded plates were seen (fig. 3a, 24 h). SAED analyses at this stage (fig. 3a, 24 h, inset) were consistent with the formation of hydroxyapatite as confirmed by FT-IR (fig. 4). In the presence of LRAP(–P)-CT, a sharp decrease in pH was again observed (fig. 2) and the minerals formed (fig. 3b) were very similar to those observed in the control. Randomly oriented rhombohedral or rounded plates of hydroxyapatite crystals were again observed at 24 h based on SAED (fig. 3b, 24 h, inset) and FT-IR (fig. 4) analyses. However, the initial pH plateau seen in the control was not observed in the presence of LRAP(–P)-CT. Under these conditions, solution pH decreased almost immediately (after 7–10 min) (fig. 2), with crystals being seen after only 10 min (fig. 3b, 5/10 min). In addition, in the presence of LRAP(–P)-CT, the pH decreased to a lesser extent than in the controls. This latter observation may

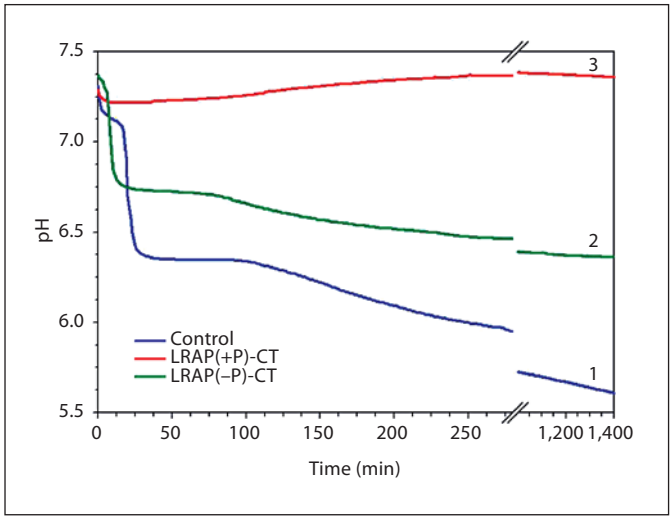

Color version available online

Fig. 2. Changes in pH as a function of time observed during mineralization experiments under conditions of spontaneous calcium phosphate precipitation over 1,400 min (~24 h) in the absence (line 1 – control) and presence of LRAP(–P)-CT (line 2) and LRAP(+P)-CT (line 3).

be due to a buffering effect by the peptide. However, in marked contrast, in the presence of LRAP(+P)-CT, after a small decrease in pH, only a slight pH change was observed for up to 1,400 min (~24 h) (fig. 2). TEM and SAED analyses showed that in the presence of LRAP(+P)-CT only spherical nanoparticles of ACP were present at 30 min (fig. 3c, 30 min, inset) and these remained with little change in size up to 24h (fig. 3c, 24 h, inset) as confirmed by FT-IR (fig. 4). ACP particles observed in the presence of LRAP(+P)-CT at 24 h were significantly smaller in diameter (29.1 ± 6.8 nm) than ACP particles seen in the controls at 5–10 min (84 ± 5.2 nm).

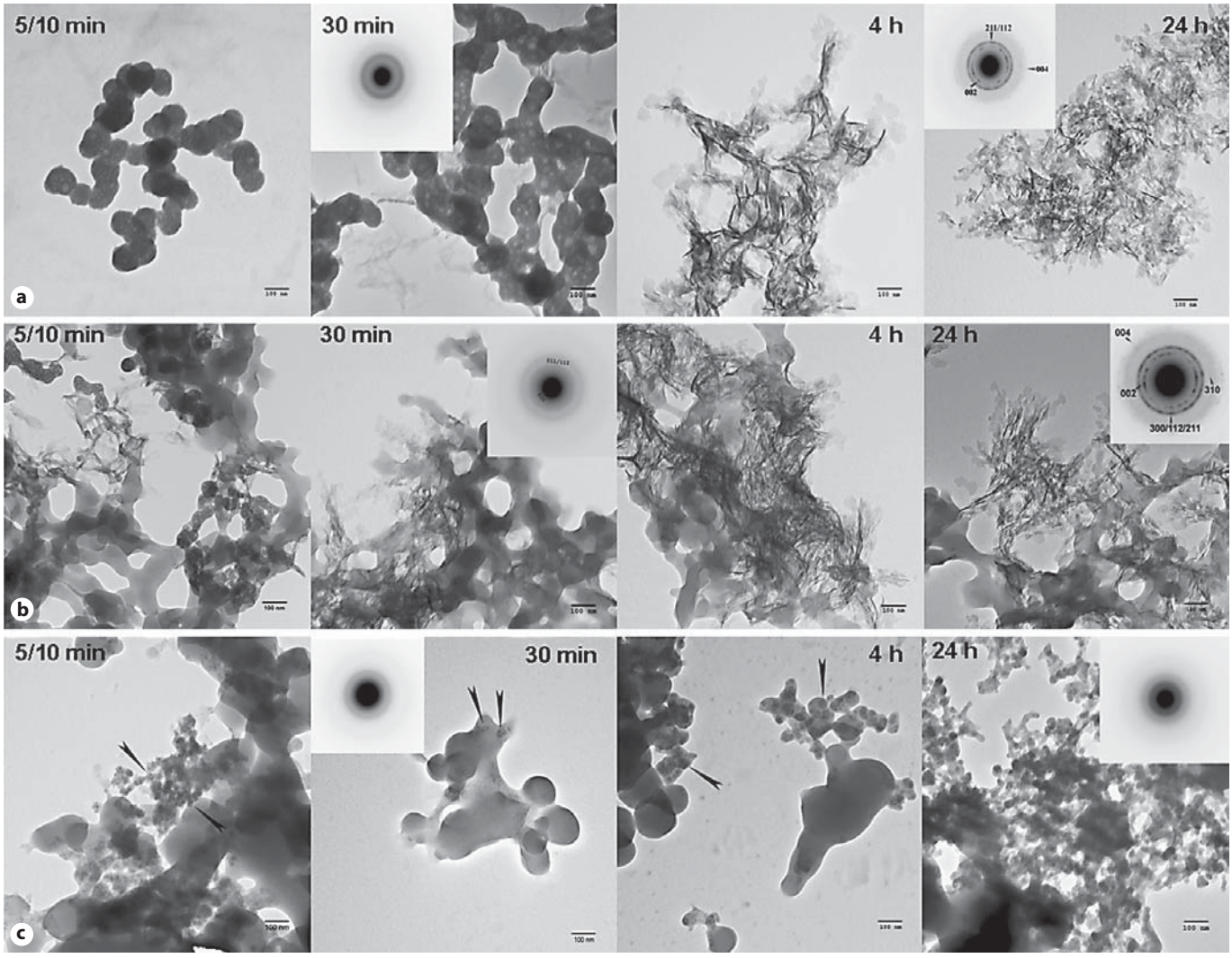

Fig. 3. TEM and SAED analyses of mineral phases formed during mineralization experiments in the absence and presence of added peptides (2 mg/ml): control (no added peptide) (**a**), LRAP(–P)-CT (**b**), and LRAP(+P)-CT (**c**). ACP was initially formed in the control (**a**) and in the presence of LRAP(+P)-CT (**c**) based on the observed (insets) SAED patterns at 30 min and the characteristic spherical morphology, whereas crystals were observed at this time in the presence of LRAP(–P)-CT (**b**) based on the observed (insets) SAED patterns at 30 min. At 4 h, randomly arranged plate-like crystals were found in the control (**a**) and in the presence of LRAP(–P)-CT (**b**). Similar structures were seen at 24 h. SAED analyses of control (**a**) and LRAP(–P)-CT (**b**) samples at 24 h were consistent with randomly oriented hydroxyapatite crystals. In contrast to these findings, in the presence of LRAP(+P)-CT (**c**), ACP remained for up to 24h. ACP particles were also observed (arrows) in the presence of LRAP(+P)-CT at 5/10 min, 30 min, and 4 h. Mineral phase identification by SAED was confirmed using FT-IR (fig. 4). Scale bars = 100 nm.

Discussion

In the present study, we have shown that LRAP(+P)-CT is an effective stabilizer of ACP, preventing its transformation into apatitic crystals, as was seen in the control and in the presence of the nonphosphorylated LRAP(–P)-CT. Similarly, we previously showed that P148, the cleaved form of the full-length porcine amelogenin P173 that lacks 25 C-terminal amino acids, also has a profound effect on spontaneous calcium phosphate formation through the stabilization of ACP [Kwak et al., 2009]. In contrast, the addition of LRAP(–P)-CT appeared to have little influence on the nature of the mineral formed in comparison to the control. However, it is apparent that ACP formation and subsequent transformation processes into randomly oriented apatitic crystals are accelerated in

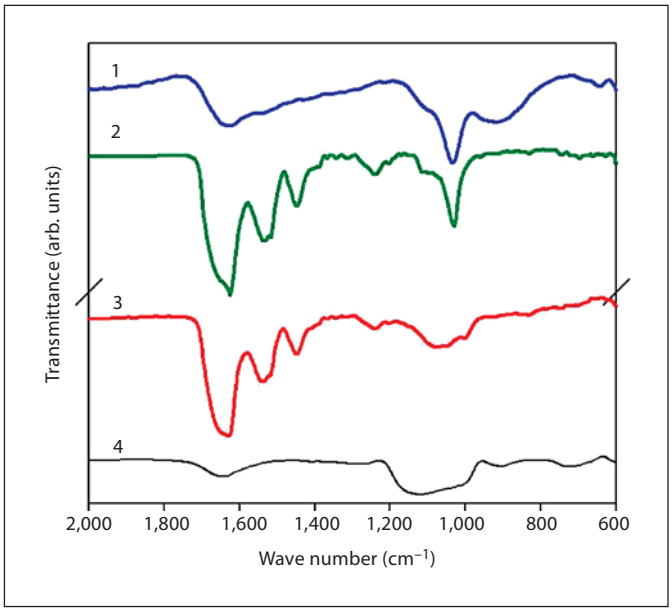

Color version available online

Fig. 4. FT-IR analyses of mineral phases formed at 24 h in the absence (line 1 – control) and presence of LRAP(–P)-CT (line 2) and LRAP(+P)-CT (line 3). As found by SAED (fig. 3), the FT-IR spectra of control samples (line 1) and products obtained in the presence of LRAP(–P)-CT (line 2) indicated the formation of hydroxyapatite ($\nu 3$ of PO_4^{3-}: 1,102 and 1,035 cm^{-1}), while the spectra of samples obtained in the presence of LRAP(+P)-CT (line 3) were consistent with ACP. Amide I (1,653 cm^{-1}), Amide II (1,553 cm^{-1}), and amino acid side chain (1,400–1,500 cm^{-1}) peaks were observed in the presence of LRAP(–P)-CT (line 2) and LRAP(+P)-CT (line 3). For comparison, a spectrum of pyrophosphate-stabilized ACP is presented (line 4). Pyrophosphate-stabilized ACP was prepared by mixing $CaCl_2$ and Na_2PO_4 with $Na_4P_2O_7$ under ambient conditions (final concentrations: 5 mM Ca, 3 mM PO_4, and 1.2 μM P_2O_7, pH ~7.1). After 30 min, the mineral suspension was centrifuged (8,000 *g* at 20°C for 5 min). The precipitate was then lyophilized at –20°C. This method is a variation of a previously described approach [Beniash et al., 2009]. arb. = Arbitrary.

the presence of the nonphosphorylated LRAP(–P)-CT peptide (fig. 3, 4). A similar finding was previously obtained using rP147 that also lacks the single phosphate group and the hydrophilic C-terminus [Kwak et al., 2009].

More importantly, our present findings indicate that the N-terminal domain found in LRAP, as in amelogenins, has the capacity to interact with forming calcium phosphate mineral phases. This finding is consistent with previous results from our laboratory that showed through in vitro mineralization studies using recombinant nonphosphorylated mouse amelogenins [Beniash et al., 2005] that, although the C-terminus of amelogenin plays an apparent role in regulating crystal organization, remaining portions of amelogenin (i.e. both the N-terminal and the central hydrophobic domains) are involved in regulating crystal shape. In the present study, we have shown that the N-terminal domain of LRAP alone has the capacity to interact with calcium phosphate mineral phases that are generated in a dynamic process. Although this effect is more apparent with the phosphorylated form of the N-terminal peptide used in the present study, these findings are consistent with the conclusion of recent NMR studies that indicate that regions of LRAP (phosphorylated and nonphosphorylated) in addition to the C-terminus are involved in hydroxyapatite binding [Shaw et al., 2004; Shaw and Ferris, 2008]. Hence, it is possible that the N-terminal domain plays a role in the regulation of the initial formation of ACP particles observed in developing enamel mineral which subsequently transform into apatitic crystals [Beniash et al., 2009]. Other molecules associated with biomineralization processes, like the highly phosphorylated osteopontin [Gericke et al., 2005] and the N-terminal domain of dentin matrix protein [Gajjeraman et al., 2007], have also been shown to stabilize ACP. Insights from the present and previous in vitro studies should aid the development of novel biomimetic approaches for enamel regeneration. In support of this idea, design approaches involving the transformation of amorphous phases to crystalline materials have been used in the development of novel bioinspired materials [Loste and Meldrum, 2001; Aizenberg et al., 2003].

Acknowledgement

This work was supported by NIDCR grant R01-DE016376 (H.C.M.).

References

Aizenberg, J., D.A. Muller, J.L. Grazul, D.R. Hamann (2003) Direct fabrication of large micropatterned single crystals. Science *299:* 1205–1208.

Aoba, T., M. Fukae, T. Tanabe, M. Shimizu, E.C. Moreno (1987) Selective adsorption of porcine-amelogenins onto hydroxyapatite and their inhibitory activity on hydroxyapatite growth in supersaturated solutions. Calcif Tissue Int *41:* 281–289.

Bartlett, J.D., J.P. Simmer (1999) Proteinases in developing dental enamel. Crit Rev Oral Biol Med *10:* 425–441.

Beniash, E., R.A. Metzler, R.S. Lam, P.U. Gilbert (2009) Transient amorphous calcium phosphate in forming enamel. J Struct Biol *166:* 133–143.

Beniash, E., J.P. Simmer, H.C. Margolis (2005) The effect of recombinant mouse amelogenins on the formation and organization of hydroxyapatite crystals in vitro. J Struct Biol *149:* 182–190.

Eanes, E.D. (2001) Amorphous calcium phosphate; in Chow, L.C., E.D. Eanes (eds): Octacalcium Phosphate. Basel, Karger, p 167.

Fincham, A.G., J. Moradian-Oldak, J.P. Simmer (1999) The structural biology of the developing dental enamel matrix. J Struct Biol *126:* 270–299.

Fukumoto, S., T. Kiba, B. Hall, N. Iehara, T. Nakamura, G. Longenecker, P.H. Krebsbach, A. Nanci, A.B. Kulkarni, Y. Yamada (2004) Ameloblastin is a cell adhesion molecule required for maintaining the differentiation state of ameloblasts. J Cell Biol *167:* 973–983.

Gajjeraman, S., K. Narayanan, J. Hao, C. Qin, A. George (2007) Matrix macromolecules in hard tissues control the nucleation and hierarchical assembly of hydroxyapatite. J Biol Chem *282:* 1193–1204.

Gericke, A., C. Qin, L. Spevak, Y. Fujimoto, W.T. Butler, E.S. Sorensen, A.L. Boskey (2005) Importance of phosphorylation for osteopontin regulation of biomineralization. Calcif Tissue Int *77:* 45–54.

Gibson, C.W., Z.A. Yuan, B. Hall, G. Longenecker, E. Chen, T. Thyagarajan, T. Sreenath, J.T. Wright, S. Decker, R. Piddington, G. Harrison, A.B. Kulkarni (2001) Amelogenin-deficient mice display an amelogenesis imperfecta phenotype. J Biol Chem *276:* 31871–31875.

Hu, J.C., Y. Hu, C.E. Smith, M.D. McKee, J.T. Wright, Y. Yamakoshi, P. Papagerakis, G.K. Hunter, J.Q. Feng, F. Yamakoshi, J.P. Simmer (2008) Enamel defects and ameloblast-specific expression in Enam knock-out/lacz knock-in mice. J Biol Chem *283:* 10858–10871.

Kwak, S.Y., F.B. Wiedemann-Bidlack, E. Beniash, Y. Yamakoshi, J.P. Simmer, A. Litman, H.C. Margolis (2009) Role of 20-kDa amelogenin (P148) phosphorylation in calcium phosphate formation in vitro. J Biol Chem *284:* 18972–18979.

Loste, E., F. Meldrum (2001) Control of calcium carbonate morphology by transformation of an amorphous precursor in a constrained volume. Chem Commun *10:* 901–902.

Mahamid, J., A. Sharir, L. Addadi, S. Weiner (2008) Amorphous calcium phosphate is a major component of the forming fin bones of zebrafish: indications for an amorphous precursor phase. Proc Natl Acad Sci USA *105:* 12748–12753.

Margolis, H.C., E. Beniash, C.E. Fowler (2006) Role of macromolecular assembly of enamel matrix proteins in enamel formation. J Dent Res *85:* 775–793.

Moradian-Oldak, J., N. Bouropoulos, L. Wang, N. Gharakhanian (2002) Analysis of self-assembly and apatite binding properties of amelogenin proteins lacking the hydrophilic C-terminal. Matrix Biol *21:* 197–205.

Moradian-Oldak, J., J. Tan, A.G. Fincham (1998) Interaction of amelogenin with hydroxyapatite crystals: an adherence effect through amelogenin molecular self-association. Biopolymers *46:* 225–238.

Nagano, T., A. Kakegawa, Y. Yamakoshi, S. Tsuchiya, J.C. Hu, K. Gomi, T. Arai, J.D. Bartlett, J.P. Simmer (2009) Mmp-20 and Klk4 cleavage site preferences for amelogenin sequences. J Dent Res *88:* 823–828.

Paine, M.L., W. Luo, D.H. Zhu, P. Bringas, Jr., M.L. Snead (2003a) Functional domains for amelogenin revealed by compound genetic defects. J Bone Miner Res *18:* 466–472.

Paine, M.L., M.L. Snead (1997) Protein interactions during assembly of the enamel organic extracellular matrix. J Bone Miner Res *12:* 221–227.

Paine, M.L., H.J. Wang, M.L. Snead (2003b) Amelogenin self-assembly and the role of the proline located within the carboxyl-teleopeptide. Connect Tissue Res *44(suppl 1):* 52–57.

Pugach, M.K., Y. Li, C. Suggs, J.T. Wright, M.A. Aragon, Z.A. Yuan, D. Simmons, A.B. Kulkarni, C.W. Gibson (2010) The amelogenin C-terminus is required for enamel development. J Dent Res *89:* 165–169.

Shaw, W.J., A.A. Campbell, M.L. Paine, M.L. Snead (2004) The COOH terminus of the amelogenin, LRAP, is oriented next to the hydroxyapatite surface. J Biol Chem *279:* 40263–40266.

Shaw, W.J., K. Ferris (2008) Structure, orientation, and dynamics of the C-terminal hexapeptide of LRAP determined using solid-state NMR. J Phys Chem B *112:* 16975–16981.

Shaw, W.J., K. Ferris, B. Tarasevich, J.L. Larson (2008) The structure and orientation of the C-terminus of LRAP. Biophys J *94:* 3247–3257.

Smith, C.E., R. Wazen, Y. Hu, S.F. Zalzal, A. Nanci, J.P. Simmer, J.C. Hu (2009) Consequences for enamel development and mineralization resulting from loss of function of ameloblastin or enamelin. Eur J Oral Sci *117:* 485–497.

Termine, J.D., A.B. Belcourt, P.J. Christner, K.M. Conn, M.U. Nylen (1980) Properties of dissociatively extracted fetal tooth matrix proteins. 1. Principal molecular species in developing bovine enamel. J Biol Chem *255:* 9760–9768.

Uchida, T., T. Tanabe, M. Fukae, M. Shimizu, M. Yamada, K. Miake, S. Kobayashi (1991) Immunochemical and immunohistochemical studies, using antisera against porcine 25 kDa amelogenin, 89 kDa enamelin and the 13–17 kDa nonamelogenins, on immature enamel of the pig and rat. Histochemistry *96:* 129–138.

Wazen, R.M., P. Moffatt, S.F. Zalzal, Y. Yamada, A. Nanci (2009) A mouse model expressing a truncated form of ameloblastin exhibits dental and junctional epithelium defects. Matrix Biol *28:* 292–303.